

Experimental Study of Thermal Performance of Coil in Shell Heat Exchanger

A. Siddique Ahmed Ghias¹, S. Vijay Ananth¹, M. Dev Anand² and G. Glan Devadhas³

¹Department of Mechanical Engineering, Agni College of Technology, Thalambur, Chennai – 603103, Tamil Nadu, India; ghias.mec@act.edu.in

²Academic Affairs, Department of Mechanical Engineering, Noorul Islam University, Kanyakumari - 629180, Tamil Nadu, India

³Department of Electronics and Instrumentation Engineering, Noorul Islam University, Kanyakumari - 629180, Tamil Nadu, India

Abstract

Background/Objectives: An experimental investigation and a numerical study of characteristics of heat transfer of coil in shell heat exchanger is performed. **Methods/Statistical Analysis:** The effects of the change in shape of tube on the heat transfer are studied here. For this, a helical coil was designed and manufactured. The difference of this study from previous ones is that the geometry of the coil is different. Existing studies used only single stretch of helical coil but in this case there are two sets of helical coil connected by a small straight tube. The heat exchanger designed is of counter flow configuration to maximize the amount of heat transferred. In the experiment, keeping constant the flow rate of shell side, the side flow rate was kept on changing and for each tube side flow rate readings were taken for different temperatures. Wilson plots were plotted for obtaining the values of convective coefficient of heat transfer. **Findings:** The experimental set up was validated; the values for friction factor and Nusselt number were within agreeable limits of theoretical values. A numerical study of the heat exchanger was carried out using FLUENT. **Applications/Improvements:** The results obtained from FLUENT supports the value obtained from the experiment.

Keywords: Counter Flow, Friction Factor, Heat Transfer, Helical Coils, Nusselt Number

1. Introduction

Equipment named heat exchanger has been constructed for heat transfer to be efficient from one medium to another. Using a solid wall the media is separated, hence mixing never happen, or they might be in contact directly. They find its application much in refrigeration and air conditioning, space heating, chemical plants, natural gas processing, petrochemical plants, power plants, petroleum refineries and sewage treatment. An internal combustion engine sounds good for considering as an example for heat exchanger where a fluid that circulates is known as engine coolant flowing via coils of radiator and flowing of air past the coils that not only cools the coolant but also heats the air which comes in. Engineers work towards

the improvement of processes and efficiency increase. These kinds of necessity arise due to the requirement of increasing the throughput of process, shoot up of profitability or locate coastal limitations. Process that utilizes equipment that causes heat transfer must commonly be enhanced for the above mentioned reasons. Few techniques have been suggested in this research to increase the performance of heat exchanger of shell and tube. Heat exchanger functioning capability rise typically says that relocating much duty or exchanger operation at nearest temperature approach. This openly translates to rise up of the overall heat transfer coefficient, U . Surface area A is associated with the overall heat transfer coefficient and duty, Q , and ΔT , difference in temperature. In every heat exchanger design references this equation is identified.

*Author for correspondence

$$Q = UA\Delta T \tag{1}$$

Transport considerations determine U . To calculate this, C is a function of the heat transfer coefficients, h , thermal conductivity of metal, k , and considerations of fouling f . When available U value overcomes the required U the exchanger typically functions perfectly.

$$U = f(h, f, K, A) \tag{2}$$

The upcoming equation that is simplified determines U , contributed the resistance of fouling, and thermal conductivity of metal are non predominant assessed against the coefficients of convective film. In addition, the area of tube inside has to be highly equivalent to the tube area that is outside.

$$= 1/h_i + 1/h_o \tag{3}$$

The above equation shows that the raise in heat transfer could be accomplished by;

- (i) Increasing ΔT (ii) Increasing A (iii) Increasing h

The only ideal and noticeable resolution for enhancing the working functionality of shell and tube heat exchanger could be for moving towards the fluids of tube and shell. The process fluids location over the tube or shell side doesn't rely on the main competent heat transfer area. Pressure is a key concern. Comparative to the shell, high-pressure fluids could be kept in the tubes, ending up in usage of least amount of construction material and a cost effective exchanger. Handling phase describes about the placement of fluids. Toggling the tube and shell side process streams are applicable when phase change does not occur in the process streams and owns just about the equivalent pressure. Heat exchanger enrichment should forever gratify the most important target in affording a cost benefit comparative to the utilization of a conventional heat exchanger. Fouling potential, reliability and safety are the factors to deal with. Passive and active are the two methods of Heat exchanger enhancement. Inserts, extended surfaces, coiled or twisted tubes, surface treatments and additives are with Passive methods. Electrostatic fields, surface vibration and suction, injection are with Active technique. Figure 1 illustrates various kinds of schematics of enhancements for the heat exchanger tubes together with the usage of inserts, fins, and twisting.

High range of variance in temperature ΔT could result in high heat flow, but ΔT is restricted frequently by constraints of process or materials. For example, high range



Figure 1. Enhancement to heat exchanger tubes.

of temperature in a nuclear reactor is maintained below the threshold value in order to prevent run away reactions and meltdown. Consequently augmented ΔT could only be accomplished through rapid decline in coolant temperature. Nevertheless this leads to the decline in nuclear reaction rate and lessen the process competence. Making the most of the heat transfer area A is a wide spread approach of progressed heat transfer, and numerous heat exchangers like radiators and plat- and frame-heat exchangers have been planned to capitalize on the heat transfer area. In automotive systems and aerospace, growth of the heat transfer area could be attained when the heat exchanger size tends to go high ending up in useless raise in weight. Heat transfer enhancement could be attained on raising up the heat transfer coefficient h involving highly equipped heat transfer techniques.

One among the passive methods in heat exchangers is by involving helically coiled tubes. The centrifugal force because of the tube curvature ends up in the development of flow that is secondary enhancing the rate of heat transfer. This results in the formation of two vortices symmetrical about a horizontal plane through the tube centre as shown in Figure 2.

When the flow of fluid is via a tube that is straight, fluid velocity is maximum at the tube centre, zero at the tube wall & symmetrically distributed about the axis of the tube. However, when the fluid flows through a curved tube, the primary velocity profile indicated above is distorted by the addition of pattern of flow that is secondary. Flow which is secondary has been generated by centrifugal action and acts in a plane perpendicular to the primary flow. Since the velocity is maximum at the tube centre, the central fluid is subjected to the maximum centrifugal action, which pushes the fluid towards the tube wall. The fluid near the tube wall moves in ward along the wall surface to replace the fluid ejected outwards.

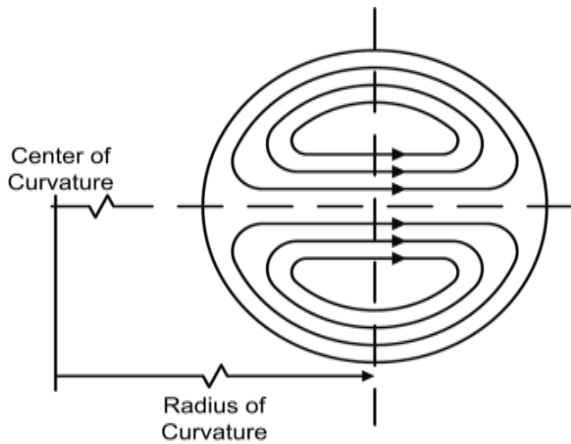


Figure 2. Flow pattern in helical coil.

2. Past Studies

Conducted an investigational learning of a heat exchanger that is of double pipe in helical shape. Testing has been carried out in sizes of both heat exchanger and both configurations of flow that is parallel and counter. Test have been carried out by keep changing mass flow rates in the tube inner and in the annulus, along with varying configuration of parallel flow and counter flow. Minute variance has been identified among the coefficients of overall heat transfer for the configuration of parallel flow and counter flow. Simultaneously rates of heat transfer rates have gone high in the counter flow configurations due to superior temperature variation an average among the two fluids. Nusselt number of annulus region was weighed against the arithmetic data. Experimental data coincides much against the arithmetic mainly for the bigger heat exchanger except only less range of divergence was identified among the small coil data which is due to disparity in the Nusselt number since the entry point varies much among the arithmetic and experimental setups. The 900 elbow utilized for connecting the experimental setup might shoot up the Nusselt number considerably in the opening region¹.

Performed an investigational learning of heat transfer convection that is mixed in a coil in heat exchanger shell corresponding to a choice of Reynolds numbers, an extend of tube to diameter of coil ratios and varying coil pitch which is dimensionless. For turbulent and laminar flow the experiments were performed within the coil. Influences of pitch of coil and diameters of tube

on coefficient of heat transfer at shell side of the heat exchanger have been noticed. Various length characteristics have been involved in numerous calculations of Nusselt number for estimating which length best apt the data. The tube diameter is identified to exhibit insignificant pressure on the coefficient heat transfer at shell-side. A negative effect on h_0 is exposed together by the coil surface area, ending up in increased coil surface concluding in coefficient of heat transfer diminution. Desperately, convection coefficient of heat transfer of shell-side shoots up parallel with the pitch of coil raise. The overall coefficient of heat transfer of heat exchanger have been learnt in order to identify the majority appropriate length of those feature upon the association among the Rayleigh and the Nusselt number and the Reynolds numbers would be achieved and lastly showing that, the corresponding heat exchanger shell-side diameter realistically make the preferred relation obvious².

Two theoretical models rely on mixed and unmixed conditions of gas flow were adopted in the idea of the performance of thermal, predicting a heat exchanger that is of spiral coil and compact. Flow rate of water effect on SCHE, on its temperature at outlet in SCHE, on temperature at outlet with hot air in SCHE were studied and compared against the SCHE performance together with cross flow heat exchangers. Two theoretical models depend upon mixed and unmixed flow of gas circumstances were built up in envisaging the spiral coil heat exchanger thermal performance. These models rely highly on mean values of heat transfer coefficients of inner and outer one which are constant. Investigational research was executed on a spiral coil laboratory model and heat exchanger obeys the rules highly along with the envisaged temperature of fluid that is cold and hot at outlet and values of effectiveness. Routine working of the heat exchanger of spiral coil could be weighed against the equivalent heat exchangers which has cross flow³.

Endeavors have been performed for researching the hydrodynamics and heat transfer hydrodynamics and characteristics of heat transfer corresponding to the tube in heat exchanger having tube that is helical at the pilot plant scale. Experiments have been performed in operational mode with counter current possessing the tube side with hot fluid and the annulus area with cold fluid. Tube at the outer has been fixed with plates that are semi-circular for supporting the inner tube and has provided turbulence of high range in annulus region as well. Along the inner and outer tube Overall heat transfer coefficient

has been calculated using Wilson plots. A commercial CFD packages has been involved for forecasting the flow and the development towards thermal in tube in heat exchanger that is helical. Factor of Friction values and Nusselt number of the tubes present inner and outer were measured against the investigational data composed in the current research and also described⁴.

Performed an investigational study for understanding the presentation of heat exchangers that is of shell and coiled tube which is helical. Mandatory parameters namely at inlet and outlet temperatures of tube's side, flow rate of fluids and shell side fluids etc was calculated involving deserved instruments. Wilson plots help in estimating overall coefficients of heat transfer of the heat exchangers. Tube and Shell sides Heat transfer coefficients were appraised appealing to the estimated over all coefficients of heat transfer. Nusselt numbers of inner side has been weighed against open literature's existing values. Coil's heat transfer coefficients of shell side holding enlarged pitches are higher than the ones possessing pitches that are small. A configuration of counter flow of the shell side Nusselt numbers are kind of higher on compared to the configuration of flow which is parallel has been noticed. To conclude, the configuration of counter flow's overall heat transfer coefficients holding 0-40 % higher compared to configuration of parallel flow is observed N⁵.

Both arithmetical and experimental investigations have been performed for understanding heat transfer that is convective from a pipe with round coiled in pattern of rectangular which is single. Heat exchangers are made up of coils present inner and outer hence flow at exterior coincides much for flowing within bundles of tube. Heat exchangers inner and outer coils are also self possessed with bends and straight portions. Experiments have been carried out for both the cases owning various outside flow planning. The outcome depicted the upshot of geometric collection with enhanced heat transfer for the arrangement that is staggered due predominantly to its added meandering characteristics of flow and enhanced assimilation of the outdoor fluid. The arithmetical and experimental outcomes depict a pipe coiling hence that fluid at exterior surge above or in bundle of tube could assist for inducing the turbulence devoid of escalating the velocity. Additionally for experimental and simulated cases even though the flow of the fluid and thermal environment varies much from each other, the outcomes actually show signs of that slighter scale heat exchangers posses appreciably enhanced heat transfer performance.

The investigational set of connections with dramatic tubes illustrates supplementary temperature that is uniform for the three dissimilar thermo couple positions at the shell side near outlet that is chiefly because of an enhanced combination of the peripheral privileged by the staggered flow preparations^{6,7}.

Discussed flow rate of experimentally achieved overall heat transfer coefficient (U) for various data in the coiled tube present inner and in region of annulus have been notified⁸.

The overall heat transfer coefficient have been noticed for varying rates of flow in the region of annulus corresponding to a flow rate which is constant in the tube that is coiled inner. Thermal profiles and velocity have been stated to visualize the development in flow the tube at inner as well as at the heat exchanger annulus⁹.

Arithmetic predictions belonging to fully built up heat transfer and hydrodynamics have been in better conformity to the experimental outcome. Model based on numerical, utilized prefers physically pragmatic circumstances, like conduction of heat within the walls of the tube. The friction factor value in the coiled tube present within conforms to the work numerically and literature data. Values of friction factor of annulus side have also identified to be conforming to the predictions numerically.

Concurrence with the experimental and numerical forecasting of Nusselt number data has been identified to conform highly less than 4% for tube present inside and 10% in coiled tube present outside, correspondingly.

3. Methodology

Helical coils of coil diameters 130mm and 65mm are used. Copper tube forms coil of 10mm ID and 12mm OD. Dimensions of helical coil are given in Table 1. Helical coil formation result in tube flattening. Experiments have been carried out with the axis of the coil vertically. Fluid enters coil from top and exits at the bottom as per the ¹⁰.

The heat exchanger shell is made of IS2606 steel and has an internal diameter of 157mm and thickness of 9mm, the height of the shell is 200mm. Flanges are connected at top and bottom of the shell and is made leak proof using gaskets.

Heater consists of a storage tank and a heater coil. The tank is made of made of steel and has dimensions of 250mm diameter and 35 mm height and has a capacity of 19liters. The heater is connected with a 3000W

Table 1. Dimensions of Helical Coils

Item	Dimension
Coil Diameter, Tube Centre to Tube Centre, (Inner) (D _{ci})	65mm
Coil Diameter, Tube Centre to Tube Centre, (Outer) (D _{co})	130mm
Straight Tube Outside Diameter, d _o	12mm
Straight Tube Inside Diameter, d _i	10mm
Approximate Number of Turns in Helical Coil (Outer)	7 Nos.
Approximate Number of Turns in Helical Coil (Inner)	9 Nos.
Curvature Ratio, d _i /D _c (Outer)	0.076
Curvature Ratio, d _i /D _c (Inner)	0.153
Axial & Heated Length of Helical Coil	4.8m
Coil Pitch, Tube Centre to Tube Centre (p)	16mm

immersion type heating coil. The temperature of water inside the heater is maintained using a thermostat.

A monobloc pump was used to pump the fluid through the experimental loop. Rotameter calibrated for readings up to 600 LPH is used; it is of flanged type and is made of acrylic body. Four J type thermocouples (iron-constantan) having a range of -40 to + 750°C were utilized in measuring the inlet and exit temperature of both hot and cold fluids. The experimental setup consists of a heater of capacity 3kW, a pump, rotameters, thermocouples, pressure gauges and heat exchanger. Connections were completed using hoses with appropriate pipe fittings. Flow regulating valves are provided at appropriate places for regulating the flow of cold and hot water. Flanged type rotameters were installed in the hot as well as cold water lines for measuring the temperature of inlet and outlet of both hot and cold water. Two pressure gauges have been connected utilizing tapings in the hot water line for measuring the drop in pressure occurring in coils.

Thermocouples were calibrated before they were installed to find out the error in them. The error calculated during calibration was taken into consideration while the actual readings were being tabulated for further proceedings.

Experiment was conducted using water as both hot and cold fluid. Hot water has been passed through the side of tube while cold water is passed through the shell side. Keeping all the valves in the tube side closed the water is heated in the heater up to a temperature of

90°C. After the water has attained the required temperature the valves are opened and water is allowed to flow through the heat exchanger. Using a series of valves the flow rate is kept constant at the required value. Now the temperature of the cold and hot water at both exit and inlet is measured and four different temperature readings are taken. Pressure drop occurring across the coils were also measured using two pressure gauges. Hot water inlet temperature is varied from 90°C to 50°C and readings are taken for every 5°C temperature difference, so particular side of shell and flow rate of tube side.

This experiment has been repeated for 6 different tube side rates keeping the flow rate of shell side constant. Tube side flow is assorted from 150 LPH to 400 LPH and the readings were taken at an interval of every 50 LPH. Similarly the experiment is repeated by varying the shell side flow rates and for each flow rates of shell side the tube side flow rate is varied 6 times and for flow rate of tube side the readings are taken by varying the hot water inlet temperature from 90°C to 50°C with 5°C intervals. The shell side mass flow rates used are 150, 250, 400, 500 LPH (0.041kg/s to 0.138kg/s). The data obtained from the experiment is tabulated and necessary calculations were made and various graphs were plotted. Hot water's heat loss amount and heat gained amount by cold water is found out using the specific heat, mass flow rate and temperature difference of the respective fluids.

$$\text{Heat lost by hot water } (Q_h) = mcp (T_{hi} - T_{ho}) \quad (4)$$

$$\text{Heat gained by cold water } (Q_c) = mcp (T_{co} - T_{ci}) \quad (5)$$

Since the heat exchanger was not fully insulated there were some losses.

$$\text{Heat lost by hot water} = \text{Heat gained by cold water} + \text{losses} \quad (6)$$

The Log Mean Temperature Difference (LMTD) was expressed as follows

$$\text{LMTD} = (\Delta T_1 - \Delta T_2) / \ln(\Delta T_1 / \Delta T_2) \quad (7)$$

$$\text{Where } \Delta T_1 = (T_{hi} - T_{co}) \quad (8)$$

$$\text{And } \Delta T_2 = (T_{ho} - T_{ci}) \quad (9)$$

The subscripts I and o represents inlet and outlet respectively.

The overall heat transfer coefficient is calculated as follows;

$$U=Q/Ax\Delta T LMTD \tag{10}$$

Where A is the area of surface of the helical coils and Q is the average of Q_h and Q_c .

Effectiveness of the heat exchanger is the ratio of heat transfer happening actual that has taken place to the possible heat transfer which is maximum that can take place; it is represented by epsilon ϵ . Maximum heat transfer takes place when the temperature of hot water at outlet is equal to the cold water temperature at inlet.

$$\epsilon = Q_{\text{actual}}/Q_{\text{Maximum}} \tag{11}$$

$$\text{Where } Q_{\text{actual}} = mc_p(T_{hi}-T_{ho}) \tag{12}$$

$$\text{And } Q_{\text{maximum}} = (mc_p)_{\text{min}} x(T_{hi}-T_{ci}) \tag{13}$$

For straight tubes the Nusselt number is calculated using Dittus – Boelter equation

$$Nu= 0.023 x Re^{0.8} x Pr^{0.4} \tag{14}$$

Where Re presents Reynolds number and Pr represents the Prandtl number and Nu represents Nusselt number.

$$Pr = \mu X C_p / \mu \tag{15}$$

$$Re = \rho X v X d / \mu \tag{16}$$

$$Nu = h X d / K \tag{17}$$

Where h is the coefficient of heat transfer of convection. Overall heat transfer coefficient U for straight tube is given by

$$U = 1/h_i + 1/h_o \tag{18}$$

Here i and o represents the tube side and shell side.

Friction factor could be determined involving the correlation proposed by Mishra and Gupta (1979)

$$f_c = 0.029 + 0.324 x [Re(d/D)^2]^{-0.25} x (D/d)^{-0.5} \tag{19}$$

Where f_c is the factor of friction of the coil, the tube diameter is d , the diameter of the helical coil is D .

After finding the friction factor we can find the head lost due to friction

$$H= f l v^2 / 2gd \tag{20}$$

$$\text{And pressure loss is equal to } pgh \tag{21}$$

Heat transfer coefficients of shell side, h_o , and for the tube side, h_p , have been estimated by the Wilson plots. It was also implemented for other heat exchanger researches.

Implementing Wilson plots, coefficient of heat transfer could be determined depending upon the difference in temperature overall and the heat transfer rate. Since measurement of temperature of tube wall is demanded here, this method was put in practices for evading the disorder of flow patterns and heat transfer when effort was put in estimating wall temperatures.

Depending upon the disconnection of the overall thermal resistance into the convective thermal resistance inside and left over thermal resistances involving in the process of heat transfer, the condensation process of overall thermal resistance in a tubes and shell condenser (R_{ov}) could be articulated as the thermal resistances sum of three that is equivalent to the tube wall (R_w), internal convection (R_i) and the external convection (R_o), as depicted in Equation (22).

$$R_{ov} = R_i + R_w + R_o \tag{22}$$

Considering straight forwardness, the thermal resistances because of the fluid fouling in Equation (22) have been avoided. Making use of the appropriate terms for the thermal resistances viewing up in Equation (22), the overall thermal resistance could be rephrased as Equation (23)

$$R_{ov} = \frac{1}{hiAi} + \frac{\ln\left(\frac{do}{di}\right)}{2\pi K_w L_w} + \frac{1}{hoAo} \tag{23}$$

Where h_o and h_i are external and internal coefficients of convection, do and d_i are the diameters of inner and outer tube, thermal conductivity of the tube is K_w , the length of the tube is L_w and area of surface of the outer and A_i and A_o , A_o and A_i , respectively.

Simultaneously, the overall thermal resistance has been utilized as a task of the coefficient of overall heat transfer submitted to the outer or inner surfaces of tube and the subsequent areas. Following this, from Equation (24) overall thermal resistance has been shown as a functionality of the coefficient of overall heat transfer which refers to the inner or outer surface ($U_i U_o$) and the area of outer or inner surface (A_o, A_i).

$$R_{ov} = 1/U_i x A_i \tag{24}$$

Brining into consideration the detailed situation of a tube and shell condenser and the equations expressed above, Wilson conceived saying when cooling liquid mass flow has been altered, and later the transformation in the overall thermal resistance might occur mostly because of

the discrepancy of the coefficient of in-tube convection, whereas left over thermal resistances are identified to be virtually constant. As a result, as expressed in Equation (25) the outside of the tubes with its thermal resistances and the wall were remarked to as an invariable.

$$R_w = R_o + C_1 \tag{25}$$

Wilson resolute saying that to handle the case of completely built up inside a circular tube the turbulent liquid flow, the convection coefficient was proportional to reduced velocity power (V_r) that end up in property of fluid and the diameter of tube discrepancy. Therefore, coefficient of convection has to be expressed as per the Equation (26).

$$H_i = C_2 \times V_r \tag{26}$$

Where a constant is C_2 , the fluid velocity that is reduced is V_r and a velocity exponent n . Followed by the thermal resistance convection associated to the tube flowing internally is proportional to $1/V_r^n$. In additional, by merging Equations (22), (25) and (26), the overall thermal resistance is identified for being a function of linear of $1/V_r^n$; which could correspond graphically in Figure 3. An examination of the association Equation (27) point to C_1 which is the intercept and $1/(C_2 \times A_i)$ is the straight line slope.

$$R_{ov} = 1/C_2 \times A_i \times 1/V_m + C_1 \tag{27}$$

Concurrently, the overall thermal resistance and the hot water velocity have been attained by experimentally quantifying the temperature at inlet (T_{in}), the temperature at outlet (T_{out}) and the temperature of cold water (T_w) at different mass flow rates (ml) of the hot water beneath the entirely built in flow which is turbulent. After that, matching to every mass flow rate for every batch of

experimental data, the overall thermal resistance is the ratio between the LMTD of the fluids and the heat flow transmitted among them, as per the Equation (28). The heat flow can be estimated from the enthalpy changed of the hot after as specified in (Eq. (28)).

$$R_{ov} = LMTD / m X c_p X (T_{out} - T_{in}) \tag{28}$$

As a result, when the exponent of velocity n value in Equation (26) is unspecified, then the overall thermal resistance experimental values could be depicted as a function of linear holding the investigational values of $1/V_m$. At this point, the straight line equation suiting the investigational data could be presumed on application of trouble free linear regression. Hence, the constants values C_1 and C_2 are determined from Equation (27) as expressed in Figure. When the C_1 and C_2 constants are calculated, then the coefficients of external and internal convection corresponding to the specified rate of flow could be appraised from the grouping of Equations (26) and (29).

$$h_o = 1/(C_1 - R_w) \times A_o \tag{29}$$

A sum of 36 Wilson plots has been plotted and the data of inner and outer coefficients of heat transfer have also been achieved. Involving these heat transfer coefficients Nusselt number has been estimated and weighed against the theoretical value to authenticate the investigational setup.

4. Numerical Analysis

Computational Fluid Dynamics (CFD) is a well known subdivision of mechanics of fluid which utilizes numerical methods and algorithms for solving and analyzing troubles which engage fluid flows. Computer program knowledge to analyze fluid flow and heat transfer in intricate geometries making available with absolute mesh flexibility that prop up 2D triangular/quadrilateral, 3D tetrahedral/ hexahedral/ pyramid/ wedge, and mixed (hybrid) meshes.

The fluent solver possess the below mentioned modeling potential;

- 2D planner, 2D Axisymmetric with swirls and 3D flows.
- Quadrilateral, triangular, hexahedral, tetrahedral, pyramid, and
- Mixed element (hybrid) meshes are promising.

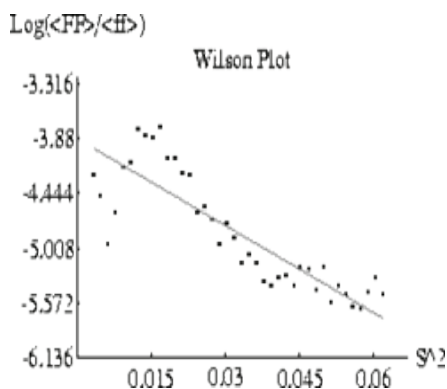


Figure 3. Wilson Plot.

- Steady state or transient flows , flows that are incompressible or compressible together with all regimes of speed could be examined
- In viscous turbulent and laminar flows.
- Non Newtonian or Newtonian flows.
- Heat transfer together with convection that is forced natural and mixed and also radiation and conjugate heat transfer.
- Capitation model and phase change models.

Fluent Package Includes

- FLUENT, the solver
- GAMBIT, pre processors for modeling geometry and generating mesh.
- T. grid a supplementary pre processor which generates meshes volume from available meshes of boundary.
- Filter (Translators) for importing volume and surface meshes from packages of CAD.

CFD analysis has been done the effects and heat transfer enhancement in a heat exchanger holding coils that are helical, with flowing hot water through the coils and cold water flowing through the shell side. This problem consists of heat exchanger which uses double helical coils made of copper instead of normal straight tubes. Drop in pressure and heat transfer can be obtained as output of

Table 2. Dimension Of Heat Exchanger

Coil Diameter, Tube Centre TO Tube Centre (inner)(Dci), mm	65
Coil Diameter, Tube Centre to Tube Centre (Outer)(Dci), mm	130
Straight Tube Outside Diameter, d_o ,mm	12
Straight Tube Inside Diameter, d_i ,mm	10
Number of Turns in Helical Coil (Outer), Nos	7
Number of Turns in Helical Coil (Inner), Nos	9
Curvature Ratio, DILDC (Outer)	0.076
Curvature Ratio, DILDC (Inner)	0.153
Axial and Heated Length of Helical Coil, m	4.8
Coil Pitch, Tube Centre to Tube – Center , mm	16
Diameter of Shell (Outer),mm	160
Diameter of Shell (Inner),mm	155
Length of Shell, mm	200

FLUENT analysis. Dimension of heat exchanger used for analysis are as follows in Table 2.

4.1 Steps Involved

4.1.1 Modeling

- The modeling is done in the software GAMBIT
- Create the geometry using GAMBIT modeling tools. 3D modeling tools are used and problem is modeled in 3D
- Specify boundary conditions
- Mesh the geometry
- First edges are meshed. Then all the surfaces are meshed using Tri/Pave scheme. Then the volume is meshed with tgrid elements.
- Export the mesh file to FLUENT

4.1.2 Analysis

- i. File
 - Read the mesh file exported from the GAMBIT.
- ii. Grid
 - Read the Grid
 - As FLUENT reads the grid file progress would be reported in the console window.
 - Check the Grid
 - FLUENT will carry out numerous checks over the mesh and progress would be reported in the console window.
 - Smooth the grid the smoothing of the grid is done until the status become ‘smoothing complete’.
 - Swap the Grid
 - The swapping of the grid is done until the number of faces swapped becomes equal to zero
 - Display the grid
 - Scale
 - Define the unit in which the grid was created.
 - Here the unit is specified as in millimeters.
- iii. Define
 - Models
- a) Specify the solver formulation to be used.
 - The solver is specified as segregated.
 - The segregated solver conventionally was utilized for mildly compressible and incompressible flows. Extraordinary practices associated with momentum discretization and continuity equations and their solution using the segregated solver have been addressed.

On preferring momentum equations and considering the steady –state continuity describing of these practices is done effortlessly.

b) Specify whether energy equation is to be used or not energy equation is selected.

c) Specify the model as viscous

Turbulence is modeled using k-ε model is a model that is semi empirical depending on transport equations model for the kinetic energy turbulence (k) along with its dissipations rate (ε). Transport equation model for k is from the equation that is exact while the transport equation model for ε has been achieved utilizing physical reasoning and abidesveryleast similarity to itsperfectcounterpart mathematically. Since our flow regime is highly turbulent we have used this model. Following equations have been used in the numerical analysis

Continuity Equation

$$\frac{\delta}{\delta x}(\rho u) + \frac{\delta}{\delta y}(\rho v) + \frac{\delta}{\delta z}(\rho w) = 0$$

Momentum Equation

$$\frac{\delta u}{\delta x}(u) + \frac{\delta u}{\delta y}(v) + \frac{\delta u}{\delta z}(w) = u \frac{1}{\rho} \frac{\delta \rho}{\delta x} \frac{\delta}{\delta x}(v + v_i) \frac{\delta u}{\delta x} + \frac{\delta u}{\delta y}(v + v_i) \frac{\delta u}{\delta y} + \frac{\delta}{\delta z}(v + v_i) \frac{\delta u}{\delta z}$$

$$\frac{\delta v}{\delta x}(u) + \frac{\delta v}{\delta y}(v) + \frac{\delta v}{\delta z}(w) = u \frac{1}{\rho} \frac{\delta v}{\delta y} \frac{\delta \rho}{\delta y} \frac{\delta}{\delta x}(v + v_i) \frac{\delta v}{\delta x} + \frac{\delta}{\delta y}(v + v_i) \frac{\delta v}{\delta y} + \frac{\delta}{\delta z}(v + v_i) \frac{\delta u}{\delta z}$$

$$\frac{\delta w}{\delta x}(u) + \frac{\delta w}{\delta y}(v) + \frac{\delta w}{\delta z}(w) = \frac{1}{\rho} \frac{\delta w}{\delta y} \frac{\delta \rho}{\delta z} \frac{\delta}{\delta x}(v + v_i) \frac{\delta w}{\delta x} + \frac{\delta w}{\delta z} \rho g$$

Energy Equation

$$\frac{\delta T}{\delta x}(u) + \frac{\delta T}{\delta y}(v) + \frac{\delta T}{\delta z}(w) = \frac{\delta}{\delta x} \frac{\delta}{\delta x}(a + a_i) \frac{\delta T}{\delta x} + \frac{\delta}{\delta y}(a + a_i) \frac{\delta T}{\delta y} + \frac{\delta}{\delta z}(a + a_i) \frac{\delta T}{\delta z}$$

Transport equation for standard K epsilon model For turbulent kinetic energy K

$$\frac{\delta}{\delta t}(\rho k) + \frac{\delta u}{\delta xi}(\rho k u_i) = \frac{\delta}{\delta xi} \left[\left(\mu + \frac{\mu_t}{\sigma_k} \right) \frac{\delta k}{\delta x_j} \right] + P_k + P_b \rho \epsilon Y_{m+s_k}$$

For Dissipation ε

$$\frac{\delta}{\delta t}(\rho \epsilon) + \frac{\delta}{\delta xi}(\rho \epsilon u_i) = \frac{\delta}{\delta x_j} \left[\left(\mu + \frac{\mu_t}{\sigma_\epsilon} \right) \frac{\delta \epsilon}{\delta x_j} \right] + C_1 \epsilon + \frac{\epsilon}{k} (P_k + C_3) \epsilon P_b C_3 \epsilon \rho \frac{\epsilon^2}{k} + S \epsilon$$

Material

a) Specify the Fluid

The fluid used is water standard properties are used

b) Specify Solid

The solid selected is copper. The default properties are used

Boundary Conditions

Boundary conditions have been pointed out as follows;

a) Inlet Conditions

Inlet mass Flow rate: varies from 0.035 to 0.13 kg/s

Temperature at section inlet: varies from 323k to 363k.

b) Outlet Conditions

Outlet section is declared as pressure outlet with pressure set as 0 Pascal(guage)

Solution

Controls

Here default under relaxation parameter is used. Pressure descritization is standard. All other descritization parameters are set second order upwind. Pressure velocity coupling selected is simple.

Monitors

Under residuals set convergence criterion to 0.0001 Plot option is checked for monitoring the convergence.

Initialize

Select the option compute from all zones so as to start the iterations.

Display Contours

Contours of temperature velocity pressure etc are selected to examine the flow.

4.2 Model Illustration

Total number of elements= 1143963. The volume meshing of the geometry is done with the help of GAMBIT. After the modeling and meshing operations various boundary types like the inlet, outlet, wall etc are defined. Now it is saved and exported.

The mesh file exported from GAMBIT is ready by the fluent software for detailed analysis. Checking and smoothing of the model is done. The boundary conditions are defined. All other conditions are set as required.

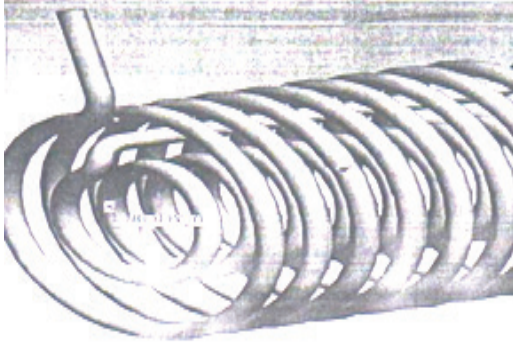


Figure 4. Coils used in heat exchanger.

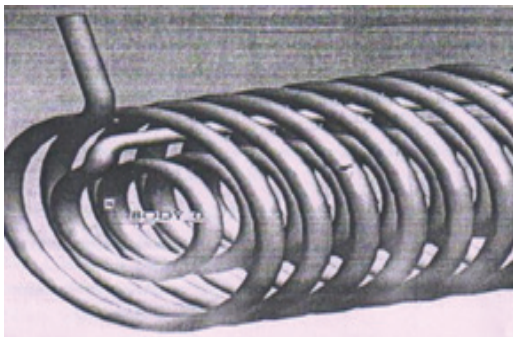


Figure 5. Meshed model of the heat exchanger.

Then iteration is done until the solution converges. The results obtained are considered for further study as shown in Figures 4 and 5.

5. Results and Discussions

The experiment was conducted by passing hot water through coils and water that is cold through the shell side, the temperatures at inlet and outlet of both the fluids that are hot and cold were measured and temperature difference with log mean, overall heat transfer coefficient Reynolds number and effectiveness were calculated. For validation of Nusselt number Wilson plot method was used.

5.1 Turbulent Flow

For turbulent flow it can use Rogers and Mayhew equation for comparing with experimental values.

$$NU = 0.023 Re^{0.8} Pr^{0.4} \delta^{0.1} \quad (17)$$

Deviation of Rogers and Mayhew equation from experimental results shown in Figures 6 and 7.

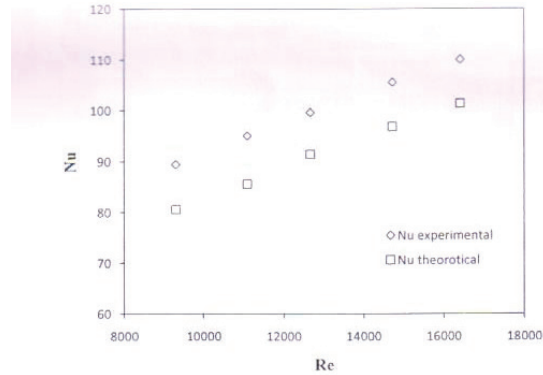


Figure 6. Data verification of helical tube for nusselt number under turbulent flow condition.

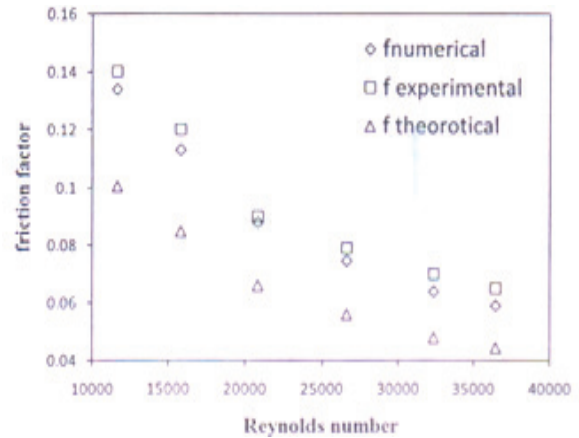


Figure 7. Data verification of helical tube for friction factor under turbulent flow condition.

Pressure drop measured during the experiment as well as the pressure drop calculated during numerical analysis were used to determine the friction factor these friction factors were compared with the friction factor obtained using the correlation proposed by Mishra and Gupta (1971).

$$F_c = 0.029 + 0.324x[Re(d/D)^2]^{0.25}x(D/d)^{-0.5}$$

The Table 3 shows the readings for tube side mass flow rate of 0.041 kg/s and shell side mass flow rate of 0.138kg/s.

The Figure 8 drawn above compares the heat lost by hot water with temperature of hot water at inlet. A comparison between the experimentally obtained results and numerically obtained results has been made. The line with rhombus marker represents the experimentally

Table 3. Data for $m_h=0.041\text{kg/s}$ and $m_c=0.138\text{kg/s}$

Thi (°C)	Tho (°C)	Tci (°C)	Tco (°C)	Del Th (°C)	Qh (kw)	Qc (kw)	U (W/m ² K)	Effectiveness (°C)	Re
90	49	30	40	41	7.175	5.83	810	70	16407
85	47	30	39	38	6.65	5.25	800	69	15566
80	45	30	38	35	6.125	4.67	790	69	14725
75	44	30	37	31	5.425	4.08	780	68	13692
70	43	30	37	27	4.725	4.08	770	66	12660
65	42	30	36	23	4.025	3.5	770	66	11874
60	40	30	35	20	3.5	2.92	760	65	11087
55	38	30	34	17	2.975	2.33	740	63	10191
50	36	30	33	14	2.45	1.75	720	62	9295

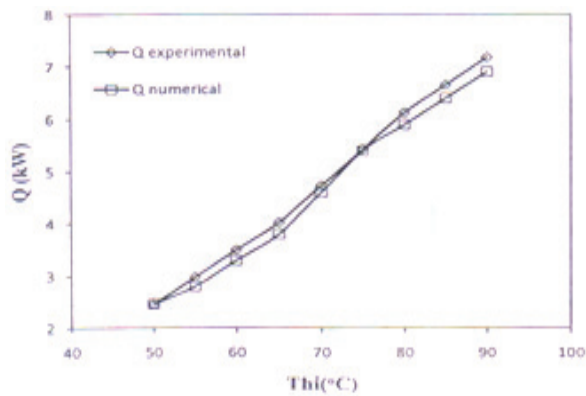


Figure 8. Variation of heat transferred with hot water temperature inlet.

obtained results while the line with square marker gives the numerically obtained results. Here as the hot water inlet temperature increase the heat transfer shoots up and the graph shows an increasing pattern. This is because as the temperature at inlet shoots up the variation in temperature among hot and cold water increase so more amount of heat can be exchanged.

The Figure 8 shows the variation of heat lost by hot water to Reynolds number. A comparison between the experimentally obtained results and numerically obtained results has been made. The line with rhombus represents the experimentally obtained results while the line with square marker gives the numerically obtained results.

The Figure 9 shows the variation between heat gained by cold water with that of hot water inlet temperature the

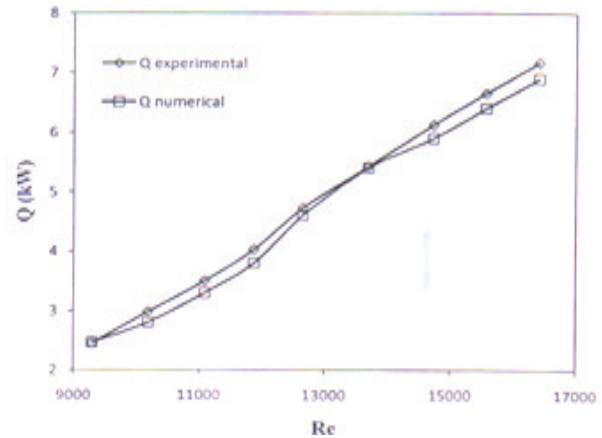


Figure 9. Variation of heat gained by cold water to hot water inlet temperature.

graph shows an increasing linear pattern because as the hot water inlet temperature increase there is more heat that is being transferred to the cold water.

The Figure 10 depicts the changes of overall heat transfer coefficient U with hot water inlet temperature which is observed from the graph that as hot water temperature at inlet increase the overall heat transfer coefficient gets rinsed. The reason for the increases is that at higher hot water inlet temperature the water has more amount of heat stored in it as a result the amount of heat transferred also goes up.

The Figure 11 exhibits the changes of overall heat transfer coefficient U with Reynolds number which could be seen from the graph that as Reynolds number rise up the overall heat transfer coefficient shoot up. As Reynolds number increases turbulence increase and there is more

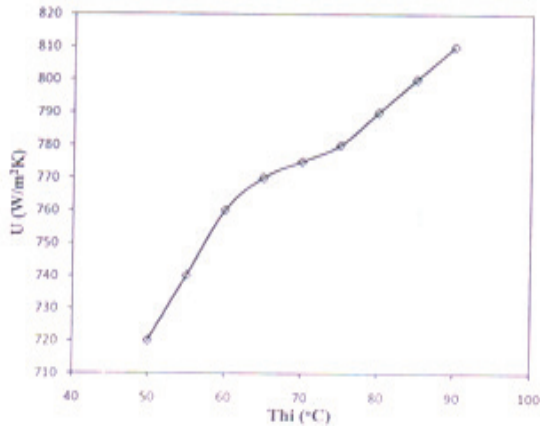


Figure 10. Variation of overall heat transfer coefficient with hot water inlet temperature.

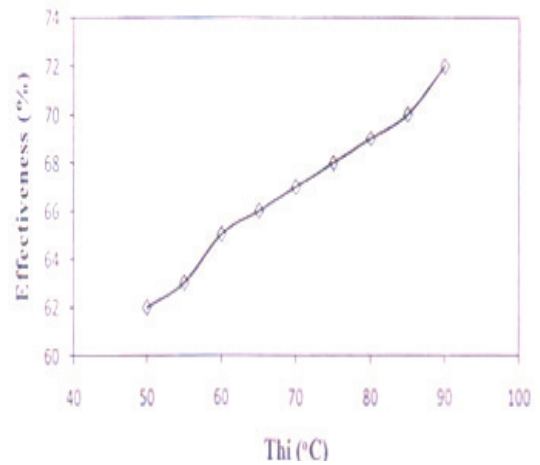


Figure 12. Variation of effectiveness with hot water inlet temperature.

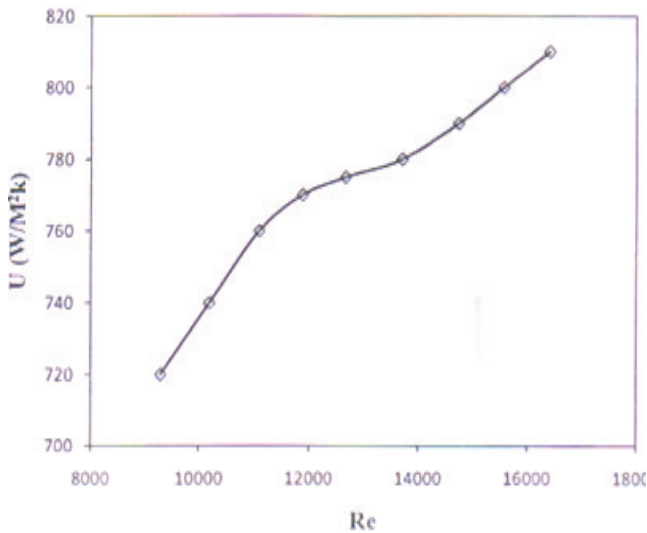


Figure 11. Variation of overall heat transfer coefficient with Reynolds number.

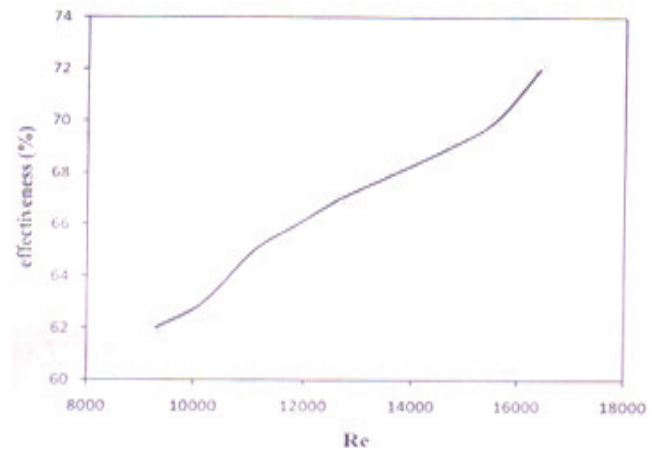


Figure 13. Comparison of heat transferred in helical coil heat exchanger with that of a straight tube heat exchanger.

efficient mixing of the fluid as a result there will be a larger heat transfer among tube wall and the fluid. Since the transfer of heat increases the convective coefficient of heat transfer also rise up as a result the overall heat transfer coefficient also increase.

The Figure 12 shows the variation of effectiveness with that of hot water inlet temperature it can be seen from the graph that as hot water temperature increase the effectiveness rise up. This is because at higher inlet temperature the temperature drop of the fluid that is hot which is elevated than at lower temperature as result the actual heat

transferred is larger at higher temperature. Even though the maximum possible heat transfer that can take place is also higher at higher inlet temperature the change in actual heat transfer is comparatively higher.

The Figure 13 depicts the association among effectiveness and Reynolds number. The graph depicts that as Reynolds number shoot up, the effectiveness also increase. The reason for this is that as turbulence increase there is more efficient mixing of the fluid as a result there will be efficient heat transfer between fluid and tube wall.

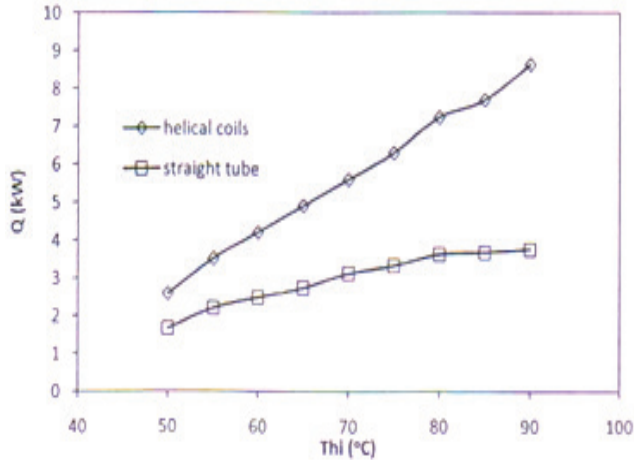


Figure 14. Comparison of heat transferred in helical coil heat exchanger with that of a straight tube heat exchanger.

The Figure 14 shows the comparison of heat transfer as hot water inlet temperature between heat exchange with helical coil and that of heat exchanger with straight tubes. It is clearly visible from the graph that heat transferred in case of helical coil is more than that of straight tube and as inlet temperature increase the difference in heat transferred increase as the inlet temperature 90°C the heat transferred in case of helical coil is almost 2.3 times that of straight tubes. The Tables 4-7 shows the readings and Figure 15-20 shows for tube side mass flow rate of 0.05, 0.069, 0.083, 0.099 kg/s and shell side mass flow rate of 0.138kg/s respectively.

The Figure 21 shows the variation of heat transferred versus the hot water inlet temperature for different shell flow rates while keeping the tube side flow rate constant. It can be seen from the graph that as shell side flow rate

Table 4. Data for $m_h=0.05\text{kg/s}$ and $m_c=0.138\text{kg/s}$

Thi (°C)	Tho (°C)	Tci (°C)	Tco (°C)	Del Th (°C)	Qh (kw)	Qc (kw)	U (W/m ² K)	Effectiveness (°C)	Re
90	53	30	41	37	8.633	6.42	876	63	20030
85	52	30	40	33	7.7	5.83	859	62	18984
80	49	30	39	31	7.233	5.25	845	61	17939
75	48	30	38	27	6.3	4.67	826	60	16689
70	46	30	37	24	5.6	4.08	814	58	15439
65	44	30	36	21	4.9	3.5	801	57	14476
60	42	30	35	18	4.2	2.92	789	56	13514
55	40	30	35	15	3.5	2.92	775	54	12422
50	39	30	34	11	2.567	2.33	756	53	11330

Table 5. Data for $m_h=0.069\text{kg/s}$ and $m_c=0.138\text{kg/s}$

Thi (°C)	Tho (°C)	Tci (°C)	Tco (°C)	Del Th (°C)	Qh (kw)	Qc (kw)	U (W/m ² K)	Effectiveness (°C)	Re
90	56	30	42	34	9.9167	7	964	57	27640
85	54	30	41	31	9.0417	6.42	956	56	26210
80	52	30	41	28	8.1667	6.42	948	55	24780
75	51	30	40	24	7	5.83	929	54	23043
70	49	30	39	21	6.125	5.25	900	52	21306
65	46	30	38	19	5.5417	4.67	885	51	19983
60	44	30	37	16	4.6667	4.08	870	49	18661
55	41	30	36	14	4.0833	3.5	856	48	17145
50	39	30	34	11	3.2083	2.33	830	47	15629

Table 6. Data for $m_h=0.083\text{kg/s}$ and $m_c=0.138\text{kg/s}$

Thi (°C)	Tho (°C)	Tci (°C)	Tco (°C)	Del Th (°C)	Qh (kw)	Qc (kw)	U (W/m ² K)	Effectiveness (°C)	Re
90	60	30	45	30	10.5	8.75	992	50	33242
85	58	30	44	27	9.45	8.17	969	49	31524
80	56	30	42	24	8.4	7	951	48	29807
75	53	30	41	22	7.7	6.42	924	47	27718
70	51	30	39	19	6.65	5.25	909	46	25629
65	49	30	38	16	5.6	4.67	898	45	24038
60	46	30	36	14	4.9	3.5	876	43	22447
55	43	30	35	12	4.2	2.92	863	42	20633
50	41	30	34	9	3.15	2.33	840	40	18819

Table 7. Data for $m_h=0.099\text{kg/s}$ and $m_c=0.138\text{kg/s}$

Thi (°C)	Tho (°C)	Tci (°C)	Tco (°C)	Del Th (°C)	Qh (kw)	Qc (kw)	U (W/m ² K)	Effectiveness (°C)	Re
90	59	30	44	31	12.658	8.17	1099	48	38660
85	58	30	43	27	11.025	7.58	1068	47	36637
80	56	30	42	24	9.8	7	1028	46	34615
75	53	30	42	22	8.9833	7	998	45	32271
70	51	30	40	19	7.7583	5.83	973	44	29928
65	49	30	40	16	6.5333	5.83	943	42	28039
60	47	30	39	13	5.3083	5.25	922	41	26150
55	44	30	37	11	4.4917	4.08	909	40	24000
50	43	30	35	7	2.8583	2.92	885	39	21850

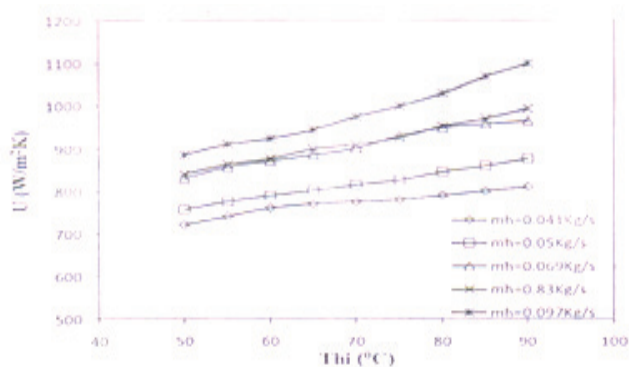


Figure 15. Variation of U with hot water inlet temperature for different mass flow rates and shell side mass flow rate of 0.138kg/s.

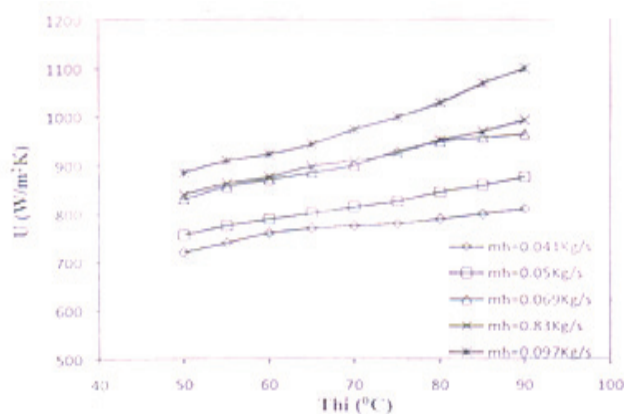


Figure 16. Variation of U with Reynolds number for different mass flow rates and shell side mass flow rate of 0.138kg/s.

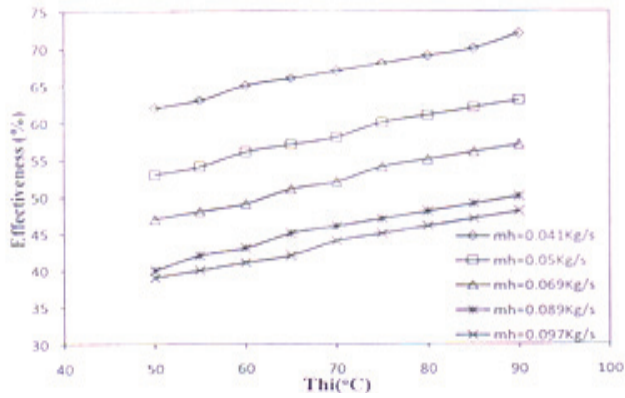


Figure 17. Variation of effectiveness with hot water inlet temperature for different mass flow rates and shell side mass flow rate of 0.138kg/s.

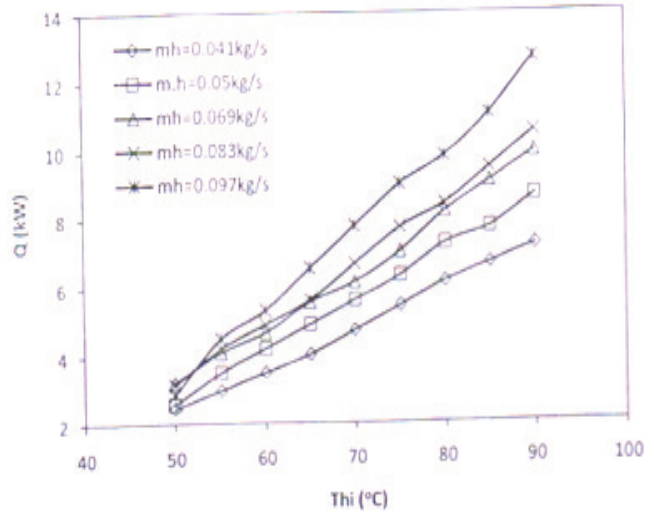


Figure 20. Variation of heat transferred with hot water inlet temperature for different hot water mass flow rates and shell side mass flow rate of 0.138kg/s.

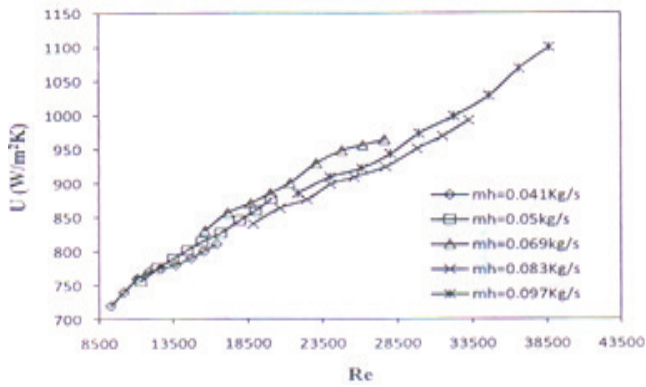


Figure 18. Variation of overall heat transfer with Reynolds number for different hot water mass flow rates and shell side mass flow rate of 0.138kg/s.

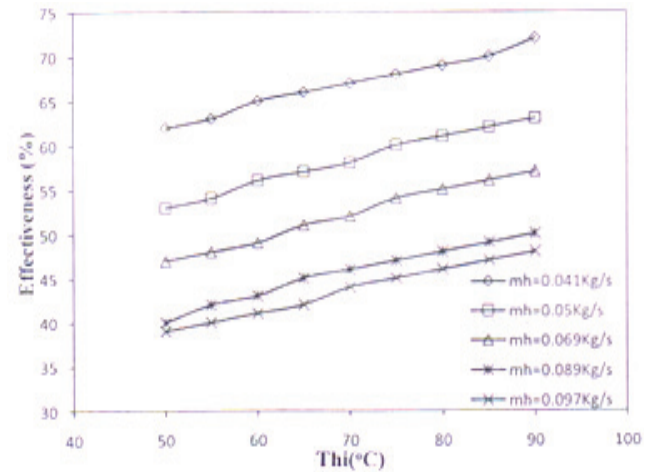


Figure 21. Variation of effectiveness with hot water inlet temperature for different hot water mass flow rates and shell side mass flow rate of 0.138kg/s.

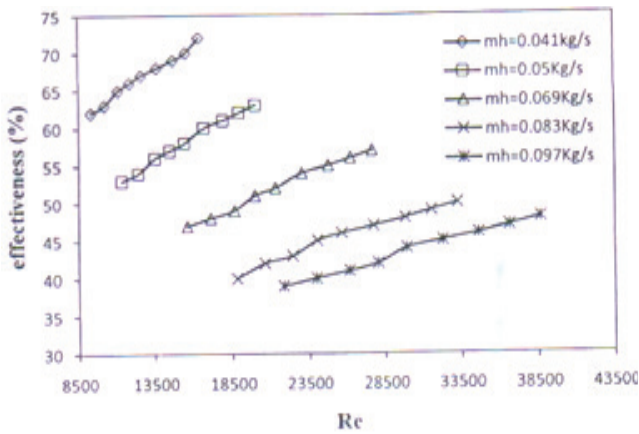


Figure 19. Variation of effectiveness with Reynolds number for different hot water mass flow rates and shell side mass flow rate of 0.138kg/s.

increase the heat capacity of the cold water also increase so it is able to take away more amount heat from the hot water.

5.2 Numerical Analysis

A model of the experimental setup was created using CAD software and was loaded into GAMBIT for meshing, after it is analyzed using FLUENT are shown in Figures 22-26.

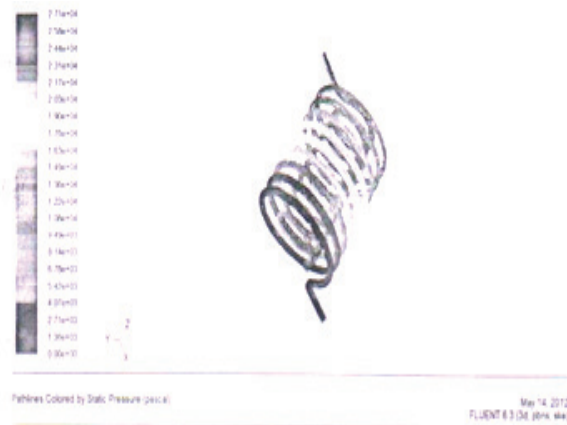


Figure 22. Pathlines showing the variation of static pressure along the coils for $m_h=0.11\text{Kg/s}$.

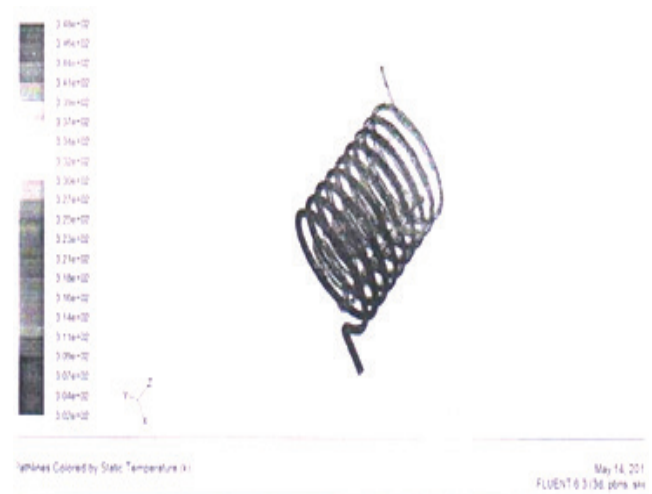


Figure 25: Pathlines showing the variation of temperature along the coils for $m_h=0.11\text{Kg/s}$.



Figure 23. Pathlines showing the variation of velocity along the coils for $m_h=0.11\text{Kg/s}$.



Figure 26: Contours showing the variation of temperature along the coils for $m_h=0.11\text{Kg/s}$.

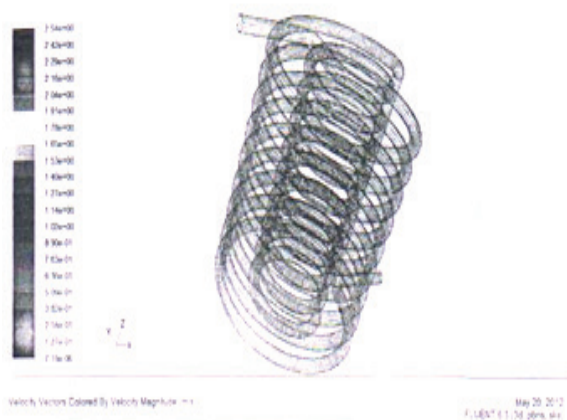


Figure 24. Contours showing the variation of velocity along the coils for $m_h=0.11\text{Kg/s}$.

6. Conclusion

Thermal Performance of coil in shell heat exchanger using helical coil was studied. The effect of variation of hot water inlet temperature variation of both the mass flow rates of tube and shell side fluid was studied and its performance was assessed against a double pipe heat exchanger with tube of same surface area. Following are the main findings of the experiment. The heat transfer rate increase as we increase the hot water inlet temperature as well as the shell side and tube side fluid flow rate. Overall heat transfer coefficient of spirally coiled heat exchanger is greater than

that of a heat exchanger using straight tube of same surface area. The effectiveness spirally coiled heat exchanger is greater than that of a heat exchanger using straight tube of same area. Heat exchanger effectiveness goes down with shoot up in tube side mass flow rate at constant shell side mass flow rate. Drop in pressure occurring in the coil is to a great extent superior than the one of tubes that is straight. Numerical data obtained closely follows the data obtained from experiment.

Further the effect of variation of coil pitch on the heat Transfer characteristics are capable of being studied. Coils curvature can be varied and the effects of change in size of inner and outer coils can be studied. The spacing between the inner and outer coils can be varied. Overall length of helical coils can be changed and its effects on pressure drop can be studied. Some heat transfer enhancement coatings can be done on the coils and its effects on heat transfer can be studied. In order to increase the turbulence in the shell side some baffles or sonic agitation can be introduced to the shell side. Detailed pressure drop studies can be undertaken and various methods of reducing the pressure drop like using of nano fluids can be studied.

7. References

1. Rennie TJ, Raghavan VGS. Experimental studies of a double-pipe helical heat exchanger. *Experimental Thermal and Fluid Science*. 2005; 29(8):919–24.
2. Ghorbani N, Taherian H, Gorji M, Mirgolbabaei H. An experimental study of thermal performance of shell and coil heat exchangers. *International Communications in Heat and Mass Transfer*. 2010; 37(7):775–81.
3. Ho JC, Wijesundera NE, Rajasekar S, Chandratilleke TT. Performance of a compact spiral coil heat exchanger. *Heat Recovery System & CHP*. 1995; 15(5):457–68.
4. Kumar V, Saini S, Sharma M, Nigam KDP. Pressure drop and heat transfer study in tube in tube helical heat exchanger. *Chemical Engineering Science*. 2006; 61(13):4403–16.
5. Shokouhmand H, Salimpour MR, Akhavan Behabadi MA. Experimental investigation of shell and coiled tube heat exchangers using Wilson plots. *International Communications in Heat and Mass Transfer*. 2008; 35(1):84–92.
6. Conte I, Peng XF. Numerical and experimental investigations of heat transfer performance of rectangular coil heat exchangers. *Applied Thermal Engineering*. 2009; 29(8-9):1799–1808.
7. Conte I, Peng XF. Numerical investigations of laminar flow in coiled pipes. *Applied Thermal Engineering*. 2008; 28(5-6):423–32.
8. Mills AF, Ganeshan V. *Heat transfer*. 2nd Ed. USA: Pearsons Education India; 2009.
9. Rajput RK. *Heat Transfer and mass transfer*, S. Chand Second Edition, 2005.
10. Cengel YA. *Heat and mass transfer-a practical approach*, USA: Tata Macgraw Hill; 2001.